Electronic Supplementary Material (ESI) for Materials Chemistry Frontiers.

Nanoporous Nitrogen-Doped Graphitic Carbon Hollow Sphere with Enhanced Electrochemical Properties

Partha Bairi[1], Kausik Sardar, Madhupriya Samanta[2,3], Kausik Chanda[1], Kalyan Kumar Chattopadhyay[1]*

[1]Department of Physics, Jadavpur University, Kolkata 700032, India

[2]School of Materials Science and Nanotechnology, Jadavpur University, Kolkata 700032, India

[3]Department of Electronics and Telecommunication Engineering, Jadavpur University, Kolkata 700032, India

Email: kalyan_chattopadhyay@yahoo.com

Table content:

1. Experimental Section:

Synthesis of PNMA and CPNMA: The nanostructured poly N-methylaniline (PNMA) was synthesized using the interfacial polymerization technique described in the literature.[15] The monomer N-methylaniline (0.4 mol) was dissolved in 100 mL water containing 1.0 g of poly (methyl vinyl ether-alt-maleic acid) by vigorous handshaking then cool it to 2 to 5 ˚C. After that, 0.6 molar 100 ml aqueous solution of pre-cooled ammonium persulfate was added slowly to the monomer solution under magnetic stirring condition and reaction still continued for another 30 min. In the course of the reaction, the temperature was kept at 0-5 °C using an ice bath. Then the reaction mixture was kept in a refrigerator for about 24 h for completion of the reaction. Then the final precipitated PNMA was separated using a centrifuge and washed with a large amount of water and finally using ethanol. To obtain the CPNMA materials we have carbonized as-synthesized solid dry PNMA using a tube furnace at different temperatures such as 800, 900, and 1000 °C under N_2 gas flow atmosphere. The 5°C/min. temperature ramp was used to reach the targeted carbonization temperature and then kept another 2 h at final temperature.

Characterization: All the FE-SEM images were taken using a Zeiss Sigma FE-SEM operating at an accelerating voltage of 5 kV. Prior to the capture of the FE-SEM images, all the carbon samples and polymer were dispersed in ethanol then drop casted on the cleaned silicon substrate and dried at 60 °C. All the dried samples were then coated with platinum (~ 2 nm) by sputtering a Hitachi S-2030 ion coater. TEM and HR-TEM images of the CPNMA-1000 sample were taken using JEOL JEM-2100 operated at 200 kV. The CPNMA-1000 sample was dispersed in ethanol by bath sonication then drop cast on a standard carbon-coated copper grid and dried at 60 °C. Powder XRD and Raman spectra of all the solid CPNMA samples were taken at room temperature using a MiniFlex 600, Rigaku, with Cu-Kα radiation and WITec alpha 300RA Raman Confocal Microscope with 532 nm diode laser respectively. The XPS data of all the CPNMA samples were obtained using SPECS HSA3500 hemispherical analyzer with a monochromatic Al-Kα x-ray source. The nitrogen gas adsorption–desorption isotherms of CPNMA-1000, CPNMA-900, and CPNMA-800 together with PNMA were measured using Quantachrome Nova1000e Instrument at liquid nitrogen temperature 77.35 K. All cyclic voltammetry and chronopotentiometry data were collected using Gamry interface 1000 electrochemical analyzer within the potential range from 0 to -1.0 V (vs. Ag/AgCl) in 2 M KOH electrolyte solution. All CPNMA modified electrodes were prepared by casting a slurry of CPNMA samples on the cleaned Nickel foam. The high viscus

slurry was prepared by dispersing 8 mg CPNMA and 1.0 mg PVDF in 350 µl water–isopropanol (3: 1) solvent containing 50 µl nafion (5 %). All the oxygen reduction reaction experiments were conducted using the Autolab instrument model number PGSTAT-M204. Prior to each measurement, 0.1 M KOH electrolyte was saturated with oxygen. The rotating disk electrode (RDE) was modified using an ink which is consists of CPNMA samples. The ink was prepared by taking 5 µL nafion solution (5 %) and CPNMA in a 95 mL water-ethanol (3:1) mixture and applied 1 h bath sonication

The kinetics of the ORR can be described by using Koutecky-Levich (K-L) equation 1 below.

$$\frac{1}{J} = \frac{1}{J_K} + \frac{1}{J_L} = \frac{1}{B\omega^{0.5}} + \frac{1}{J_K} \quad \ldots\ldots\ldots\ldots\ldots\ldots\ldots\ldots\ 1$$

$$B = 0.62nFC_0\,(D_0)^{2/3}\vartheta^{-1/6} \quad \ldots\ldots\ldots\ldots\ldots\ldots\ 2$$

$$J_K = nFKC_0 \quad \ldots\ldots\ldots\ldots\ldots\ldots\ldots\ldots\ldots\ldots\ 3$$

Where J, J_K and J_L are the measure current density, the kinetic and diffusion-limiting current density of the electrode. The angular velocity of the disk is ω (ω = 2πN, N is the linear rotation speed), n is the number of electrons transferred in oxygen reduction at the cathode, F is the Faraday constant (F = 96485 $Cmol^{-1}$), C_0 is the bulk concentration of oxygen ($C_0 = 1.2 \times 10^{-3}$ mol L^{-1}), ν is the kinematic viscosity of the electrolyte (ν = 0.1 $m^2\ s^{-1}$), diffusion coefficient D_0 (1.9×10^{-5} cm s^{-1}), and K is the electron transfer rate constant. All the parameters are valid when we have performed ORR in 0.1 M KOH as an electrolyte.

2. **Table S1**: Nitrogen adsorption-desorption results of all the CPNMA samples

Sample	Total BET surface area (m^2g^{-1})	Micropore surface area (m^2g^{-1})	Average pore diameter (nm)	Total pore volume (ccg^{-1})	Micro pore volume (ccg^{-1})
CPNMA-800	15.4	0	6.6	0.003	0
CPNMA- 900	227.4	192.5	2.4	0.14	0.1
CPNMA-1000	545.1	498.4	2.3	0.31	0.27

3. **Table S2**: Various nitrogen doped carbon synthesis and comparison their specific surface area and total atomic percentage of doped-nitrogen

Carbons	Precursor	Carbonization temperature °C	Total BET surface area m^2g^{-1}	Total atomic % of Nitrogen	References
N,F-Carbon-1000	Polytetrafluoroethylene/ polyaniline	1000	838	1.74%	S1
NC-900	Polypyrrole and KOH activation	900	1450	2.8	S2
PNCNT	Polypyrrole and KOH activation	650	1765	4.36	S3
PNHCS	polyaniline	600	213	6.7	S4
CT	polyaniline	500	312	1.2	S5
PDMC-900	polyaniline	900	-	4.39	S6
CX1000	Polypyrrole (silica xerogel as template)	1000	1480	3.55	S7
NCNFs	polypyrrole + polyacrylonitrile	900	34.5	12.53	S8
G-CBP-a	polyaniline + Amine functionalized GO	1000	362.9	5.3	S9
C-PANI	polyaniline	800	322	5.8	S10
MEP-NC850	polyaniline	850	1341.12	4.26	S11
NCM-700	poly(1,5-diaminonapthalene)	700	403	5.94	S12
Hollow PANI	polyaniline	800	-	4.03	S13
N-CNTs(1000)-1.5	Polyaniline halloysite-template	1000	261	4.87	S14
CTS-4-700	Carbazole-terephthalaldehyde	700	1226	2.5	S15
CPNMA-800	poly(N-methylaniline)	800	15.4	8.94	This Work
CPNMA-900	poly(N-methylaniline)	900	227.4	4.82	This Work
CPNMA-1000	poly(N-methylaniline)	1000	545.1	3.53	This Work

4. **Table S3**: ORR results of all the CPNMA samples obtained from LSV data taken using RDE at a rotating speed of 1600 rpm

Samples	Onset potential	$E_{0.5}$	Limiting current density	Number of electron transfer	Tafel slope mV/Decade
CPNMA-1000	0.87	0.73	-3.32	2.53	67.1
CPNMA-900	0.85	0.69	-2.68	2.58	55.9
CPNMA-800	0.80	0.65	-3.41	3.4	58.1

5. **Table S4**: Various nitrogen-doped carbon and comparison their specific ORR activity

Samples	Onset potential (V)	$E_{0.5}$	Cathodic peak potential (V)	Reference
Co-P,N-CNT	0.916	0.803	0.798	S16
2D-hBN/RGO	0.798	-	-	S17
N-CNTs(900)-1	-	0.769	0.74	S18
N-,O-,S-OMCs	0.96	0.74	0.75	S19
PDMC-800	0.71	-	0.94 V	S20
NHPC1:3-900	0.87	0.73	0.82	S21
Carbon-L	0.86	0.7	0.73	S22.
NGSH	0.88	0.7	-0.3	S23
NCNC	0.87	0.78	-	S24
CPNMA-1000	0.87	0.73	0.72	This work
CPNMA-900	0.85	0.69	0.64	This work
CPNMA-800	0.80	0.65	0.66	This work

6. Table S5: Various carbon materials and comparison their specific capacitance

Carbon Materials	Specific capacitance (Fg^{-1})	Scan rate/Current density	Electrolyte	Reference
PNHCS (N-doped carbon)	213	0.5 A g^{-1}	6 M KOH	45
NHCNs-750 (N-doped carbon)	210.1	5 mV s^{-1}	6 M KOH	46
HPCT-4 (N-doped carbon)	365.9	0.1 A g^{-1}	6 M KOH	47
NDC (N-doped carbon)	187.1	1 A g^{-1}	1 M H_2SO_4	48
NC-900 (N-doped carbon)	190	2 mV s-1	1.5 M MeEt3NBF4/PC	49
CNFs@polypyrrole (N-doped carbon)	202	1 A g^{-1}	6 M KOH	50
N-CS (N-doped carbon)	191.9	0.1 A g^{-1}	1 M H_2SO_4	51
Zn-TA-40%-90	271	0.2 A g^{-1}	6 M KOH	52
Boron-doped carbon	0.26 228	2 mVs^{-1} 1 mVs^{-1}	6 M KOH 1 M H_2SO_4	53 54
Graphene aerogel	175 128	10 mVs^{-1} 50 mA g^{-1}	5 M KOH 6 M KOH	55 56
Carbon nanotube	180 102	- 100 Hz	7.5 N KOH 38 wt % H_2SO_4	57 58
Activated carbon	292.2 261.3	5 mVs^{-1} 1 A g^{-1}	1 M H_2SO_4	59
Mesoporous fullerene crystals	172 141 6.4	0.5 A g^{-1} 0.5 A g^{-1} 5 mV s¹1	6 M KOH Na_2SO_4 1 M H_2SO_4	60 61 62
CPNMA-1000	301.8 332.4	10 mVs^{-1} 2 Ag^{-1}	2 M KOH	This work
CPNMA-900	176.2 130	10 mVs-1 2 Ag-1	2 M KOH	This work
CPNMA-800	54.9 20.8	10 mVs-1 2 Ag-1	2 M KOH	This work

7. SEM images of PNMA and CPNMA-1000

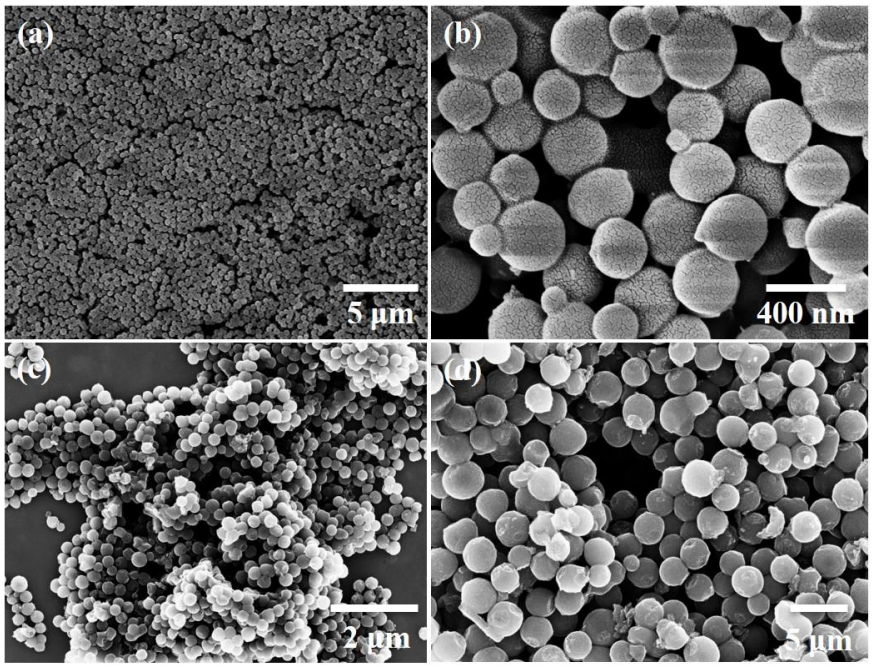

Figure S1: FESEM images of PNMA (a, b) and CPNMA-1000 (c, d)

8. The SEM images of CPNMA-900 and CPNMA-800

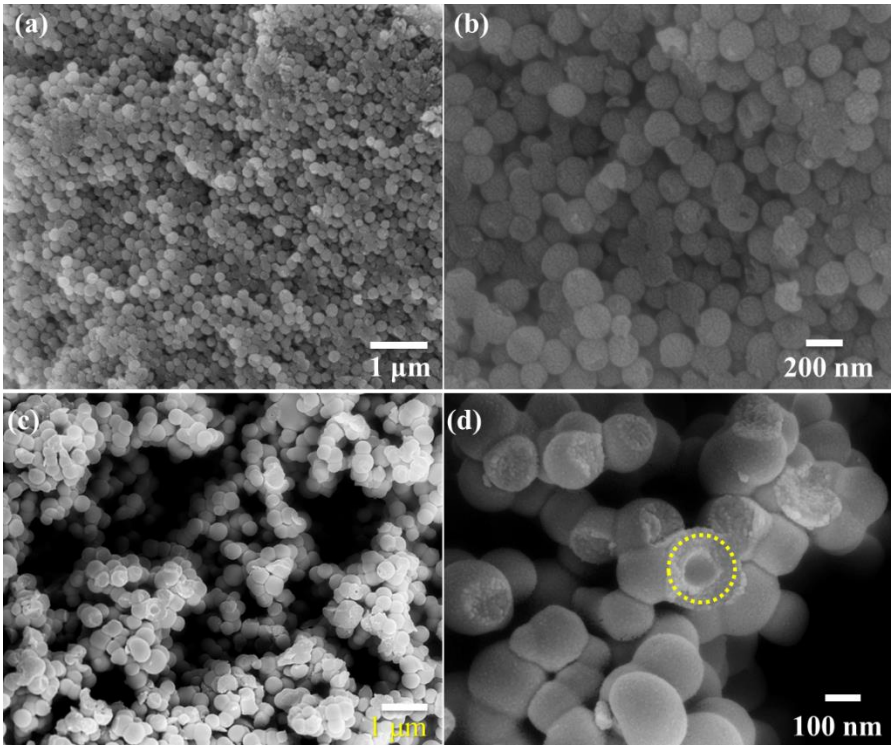

Figure S2: SEM images of CPNMA-900 and CPNMA-800 samples

9. Nitrogen adsorption-desorption plot

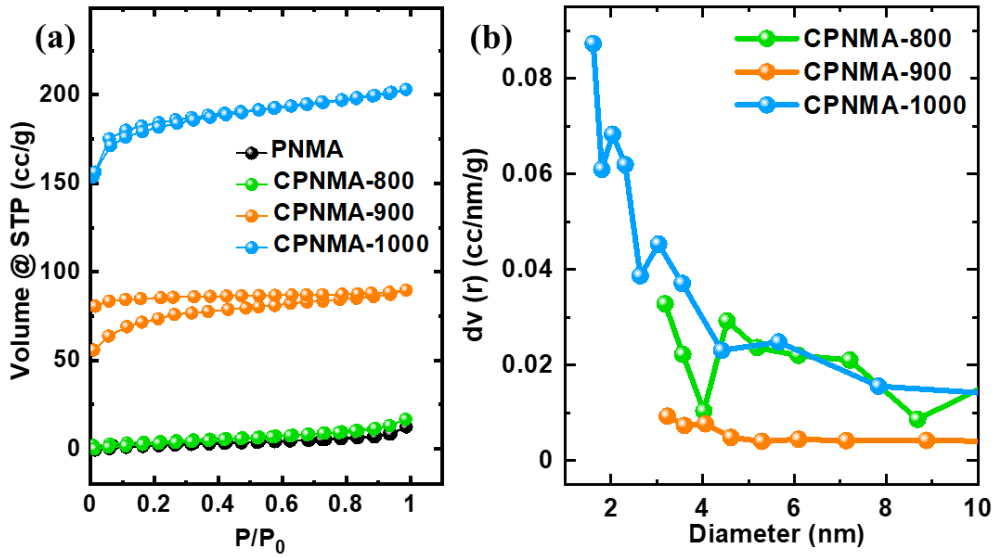

Figure S3: Nitrogen adsorption-desorption isotherm (a) and pore diameter distribution (b) of CPNMA carbons

10. XPS survey plot

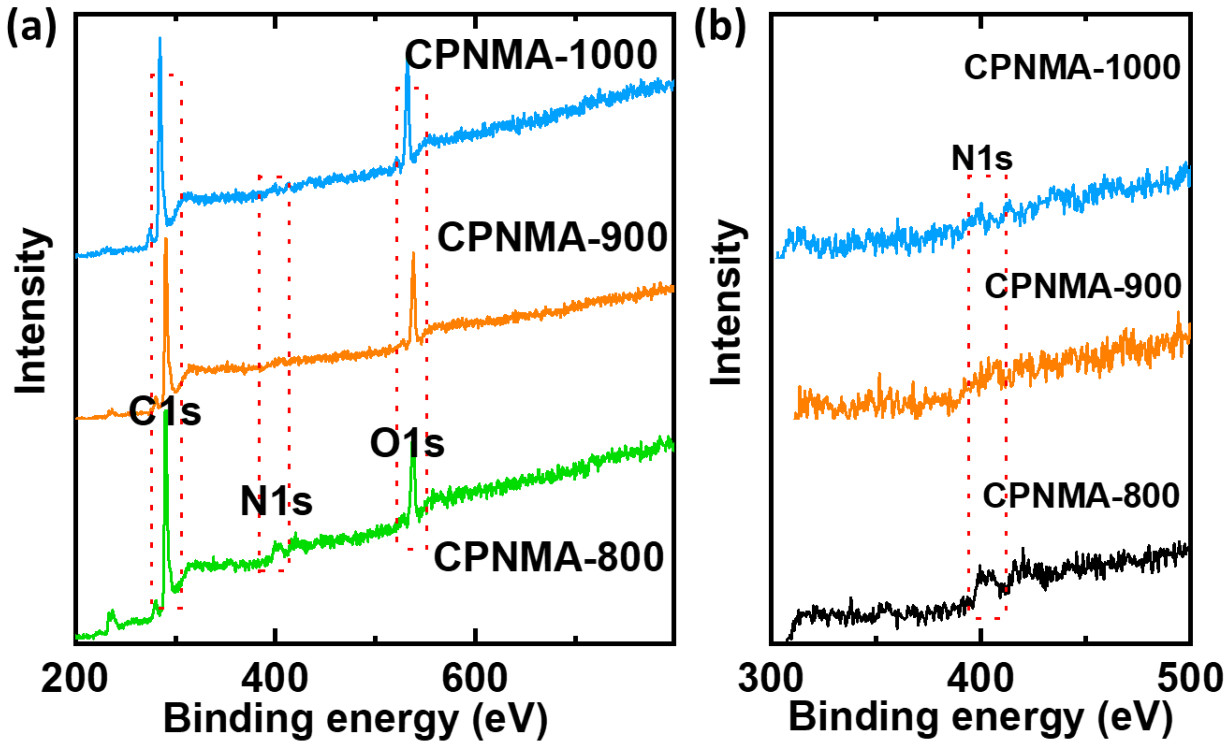

Figure S4: XPS survey plot of CPNMA samples

11. Percentage of graphitic nitrogen vs carbonization temperature plot

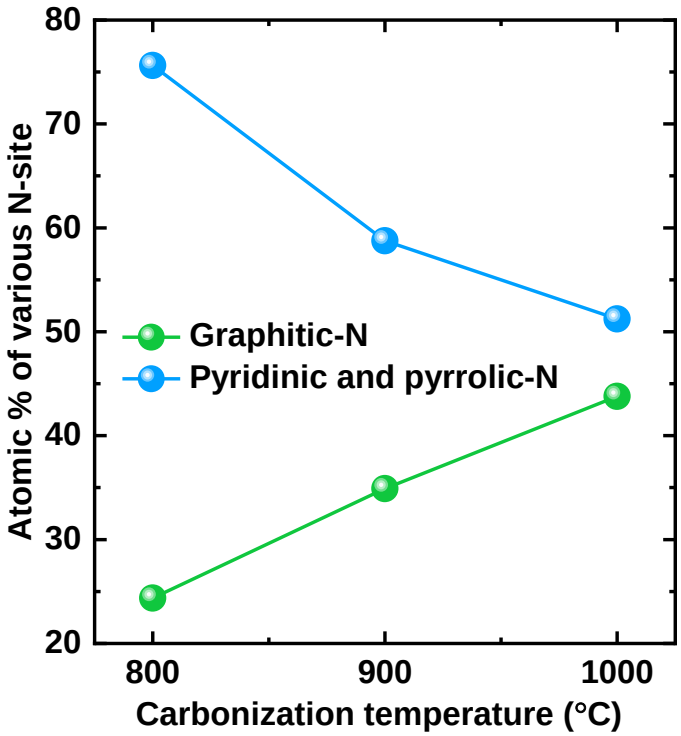

Figure S5: Atomic % of various nitrogen species vs carbonization temperature plot

12. Deconvolution plot of O1s XPS spectra

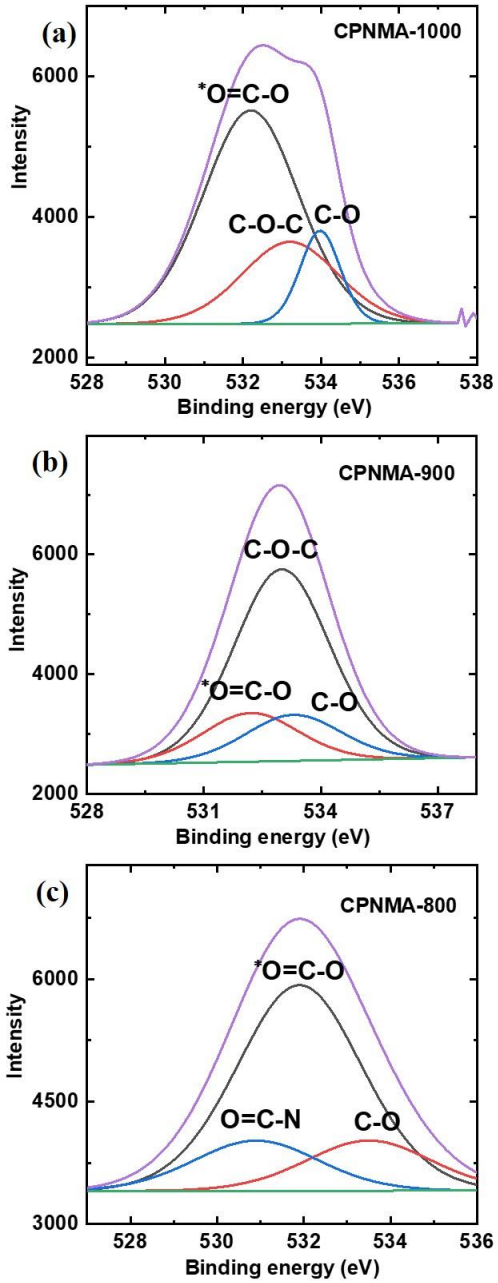

Figure S6: Deconvolution of high resolution O1s XPS spectra of (a) CPNMA-1000, (b) CPNMA-900) and (c) CPNMA-800 respectively

13. LSV and K-L plot

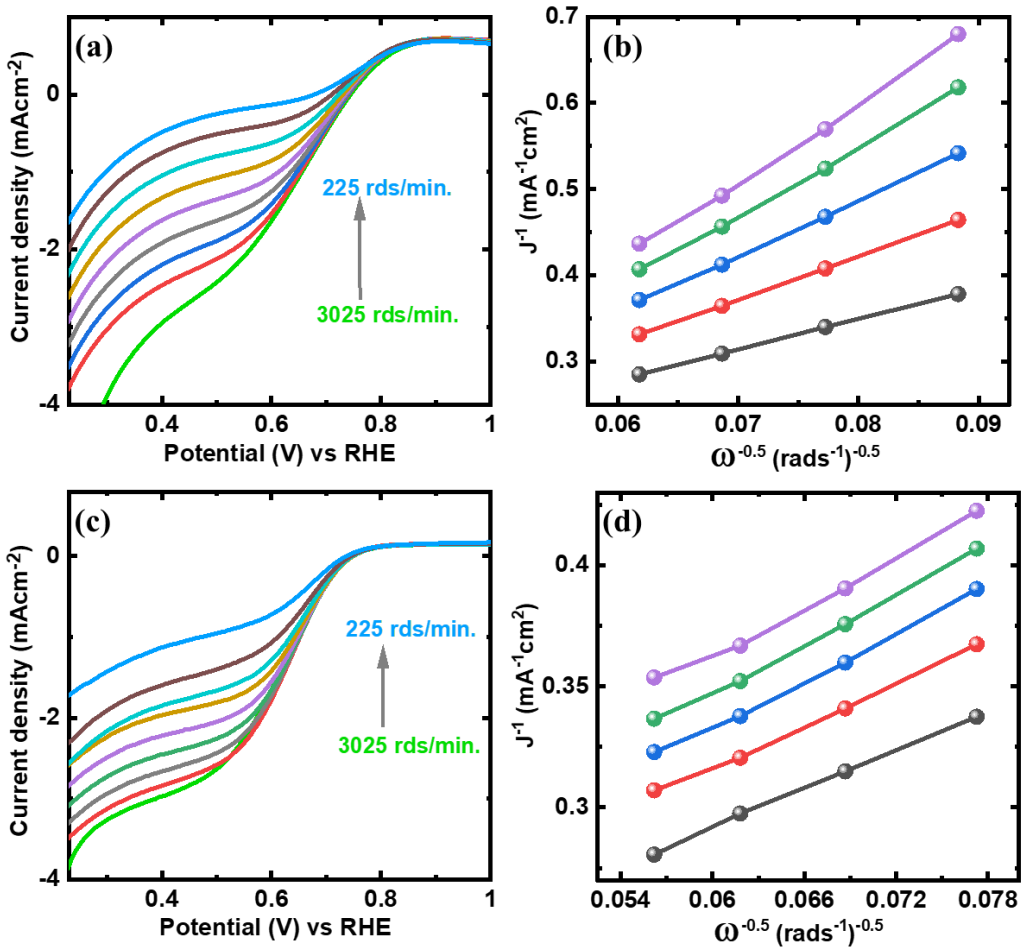

Figure S7: (a, c) LSV plot and (b, d) corresponding K-L plot of CPNMA-900 and CPNMA-800 respectively

14. References:

1. Y. Lv, L. Yang and D. Cao, Nitrogen and Fluorine-codoped Porous carbons as efficient metal-free electrocatalysts for oxygen reduction reaction in fuel cells, *ACS Appl. Mater. Interfaces*, 2017, **9**, 32859−32867.
2. J. Zhu, Y. Xu, Y. Zhang, T. Feng, J. Wang, S. Mao and L. Xiong, Porous and high electronic conductivity nitrogen-doped nanosheet carbon derived from polypyrrole for high-power supercapacitors, *Carbon*, 2016, **107**, 638-645.
3. G. Xu, B. Ding, P. Nie, L. Shen, J. Wang and X. Zhang, Porous nitrogen-doped carbon nanotubes derived from tubular polypyrrole for energy-storage applications, *Chem. Eur. J.*, 2013, **19**, 12306 – 12312.
4. J. Han, G. Xu, B. Ding, J. Pan, H. Dou and D. R. M. Farlane, Porous nitrogen-doped hollow carbon spheres derived from polyaniline for high performance supercapacitor, *J. Mater. Chem. A*, 2014, **2**, 5352–5357.
5. T. Zhu, J. Zhou, Z. Li, S. Li, W. Si and S. Zhuo, Hierarchical porous and N-doped carbon nanotubes derived from polyaniline for electrode materials in supercapacitors, *J. Mater. Chem. A*, 2014, **2**, 12545–12551.
6. R. Silva, D. Voiry, M. Chhowalla and T. Asefa, Efficient metal-free electrocatalysts for oxygen reduction: polyaniline-derived N- and O-doped mesoporous Carbons, *J. Am. Chem. Soc*., 2013, **135**, 7823−7826.
7. M. Sevilla, L. Yu, T. P. Fellinger, A. B. Fuertes and M.-M. Titirici, Polypyrrole-derived mesoporous nitrogen-doped carbons with intrinsic catalytic activity in the oxygen reduction reaction, *RSC Adv*., 2013, **3**, 9904–9910.
8. J, Guo, J, Liu, H, Dai, R, Zhou, T, Wang, C, Zhang, S, Ding and H.-G. Wang, Nitrogen doped carbon nanofiber derived from polypyrrole functionalized polyacrylonitrile for applications in lithium-ion batteries and oxygen reduction reaction, *J. Colloid Interface Sci.*, 2017, **507**, 154–161.
9. Y. Zhang, X. Zhuang, Y. Su, F. Zhang and X. Feng, Polyaniline nanosheet derived B/N co-doped carbon nanosheets as efficient metal-free catalysts for oxygen reduction reaction, *J. Mater. Chem. A*, 2014, **2**, 7742–7746.
10. N. Gavrilov, I. A. Pasti, M. Mitric, J. T.-Sejdi, G. C.-Marjanovic and S. V. Mentus, Electrocatalysis of oxygen reduction reaction on polyaniline-derived nitrogen-doped carbon nanoparticle surfaces in alkaline media, *J. Power Sources*, 2012, **220**, 306-316.

11. F. Zhou, G. Wang, F. Huang, Y. Zhang and M. Pan, Polyaniline derived N- and O-enriched high surface area hierarchical porous carbons as an efficient metal-free electrocatalyst for oxygen reduction, *Electrochim. Acta*, 2017, **257,** 73–81.
12. D. Zhu, Y. Wang, L. Gan, M. Liu, K. Cheng, Y. Zhao, X. Deng and D. Sun, Nitrogen-containing carbon microspheres for supercapacitor electrodes, *Electrochim. Acta*, 2015, **158,** 166–174.
13. S. Xing, L. Chen, L. Huang, T. Wang, X. Yu, Y. Zhang and Y. Xing, One-step synthesis of hollow nanostructured aniline oligomers and their derived nitrogen doped carbon, *Synthetic Metals*, 2017, **227**, 170–176.
14. W. Liu, Q. Ru, S. Zuo, S. Yang, J. Han and C. Yao, Controllable synthesis of nitrogen-doped carbon nanotubes derived from halloysite-templated polyaniline towards nonprecious ORR catalysts, *Appl. Surf. Sci*., 2019, **469**, 269–275.
15. N. Deka, J. Barman, J. Deka, K. Raidongia and G. K. Dutta, Microporous organic polymer-derived nitrogen-doped porous carbon spheres for efficient capacitive energy storage, *Chem. Electro. Chem*, 2019, **6**, 3327–3336.
16. S. Guo, P. Yuan, J. Zhang, P. Jin, H. Sun, K. Lei, X. Pang, Q. Xu and F. Cheng, Atomic-scaled cobalt encapsulated in P, N-doped carbon sheaths over carbon nanotubes for enhanced oxygen reduction electrocatalysis under acidic and alkaline media, *Chem. Commun.*, 2017, **53**, 9862-9865.
17. I. M. Patil, M. Lokanathan and B. Kakade, Three-dimensional nanocomposite of reduced graphene oxide and hexagonal boron nitride as an efficient metal-free catalyst for oxygen electroreduction, *J. Mater. Chem. A*, 2016,**4**, 4506-4515.
18. W. Liu, Q. Ru, S. Zuo, S. Y. Jie, Han and C. Yao, Controllable synthesis of nitrogen-doped carbon nanotubes derived from halloysite-templated polyaniline towards nonprecious ORR catalysts, *Appl. Surf. Sci*., 2019, **469**, 269–275.
19. Y. Meng, D. Voiry, A. Goswami, X. Zou, X. Huang, M. Chhowalla, Z. Liu, and T. Asefa, N-, O-, and S-tridoped nanoporous carbons as selective catalysts for oxygen reduction and alcohol oxidation reactions, *J. Am. Chem. Soc*., 2014, **136**, 39, 13554–13557.
20. R. Silva, D. Voiry, M. Chhowalla and T. Asefa, Efficient metal-free electrocatalysts for oxygen reduction: polyaniline-derived N- and O-doped mesoporous Carbons, *J. Am. Chem. Soc*., 2013, **135**, 21, 7823–7826.